

**Key Points:**

- Summertime Southern Annular Mode anomalies modulate the seasonal cycle of sea ice extent
- Positive values of the summertime Southern Annular Mode are followed by increased sea ice extent during autumn
- The negative Southern Annular Mode during the 2016/2017 austral summer contributed to the record minimum sea ice extent in March 2017

**Supporting Information:**

- Supporting Information S1

**Correspondence to:**

E. W. Doddridge,  
ewd@mit.edu

**Citation:**

Doddridge, E. W., & Marshall, J. (2017). Modulation of the seasonal cycle of Antarctic sea ice extent related to the Southern Annular Mode. *Geophysical Research Letters*, 44, 9761–9768.  
<https://doi.org/10.1002/2017GL074319>

Received 26 MAY 2017

Accepted 27 AUG 2017

Accepted article online 1 SEP 2017

Published online 5 OCT 2017

## Modulation of the Seasonal Cycle of Antarctic Sea Ice Extent Related to the Southern Annular Mode

Edward W. Doddridge<sup>1</sup> and John Marshall<sup>1</sup>

<sup>1</sup>Earth, Atmospheric and Planetary Science, Massachusetts Institute of Technology, Cambridge, MA, USA

**Abstract** Through analysis of remotely sensed sea surface temperature (SST) and sea ice concentration data, we investigate the impact of winds related to the Southern Annular Mode (SAM) on sea ice extent around Antarctica. We show that positive SAM anomalies in the austral summer are associated with anomalously cold SSTs that persist and lead to anomalous ice growth in the following autumn, while negative SAM anomalies precede warm SSTs and a reduction in sea ice extent during autumn. The largest effect occurs in April, when a unit change in the detrended summertime SAM is followed by a  $1.8 \pm 0.6 \times 10^5 \text{ km}^2$  change in detrended sea ice extent. We find no evidence that sea ice extent anomalies related to the summertime SAM affect the wintertime sea ice extent maximum. Our analysis shows that the wind anomalies related to the negative SAM during the 2016/2017 austral summer contributed to the record minimum Antarctic sea ice extent observed in March 2017.

### 1. Introduction

The Southern Annular Mode (SAM) is the dominant mode of variability in the extratropical Southern Hemisphere (Gong & Wang, 1999; Thompson & Wallace, 2000). The SAM is the leading empirical orthogonal function in a number of variables: geopotential height, surface temperature, surface pressure, and zonal winds (Thompson & Wallace, 2000). Positive SAM anomalies are associated with a strengthening and a poleward shift of the midlatitude westerlies over the Southern Ocean (Thompson & Wallace, 2000). The observational record shows a statistically significant increase in SAM over the most recent decades (Marshall, 2003). There is a seasonal bias to this increase; the effect is largest in the austral summer (December–January–February). This seasonality is likely linked to the depletion of stratospheric ozone over Antarctica (Polvani et al., 2011). The seasonal SAM index from 1970 is shown in Figure 1a along with the trend line for the summertime SAM.

The anomalous westerly winds over the Southern Ocean associated with SAM perturbations lead to anomalies in the sea surface temperature (SST). These temperature anomalies are largely caused by additional Ekman transport in the upper ocean (Ferreira et al., 2015; Purich et al., 2016), but atmospheric feedbacks also play an important role (Seviour et al., 2016; Seviour et al., 2017). The anomalous Ekman transports converge or diverge at approximately 55°S for positive and negative SAM anomalies, respectively (Kostov et al., 2017). During positive SAM anomalies, the upper ocean south of the convergence is cooled by the transport of cold water northward; north of the convergence the SST is warmed. The anomalous January winds associated with a  $+1\sigma$  summertime SAM are shown in Figure 1b.

Recent reviews have clearly articulated the complexity of the ocean–ice–atmosphere system in the Southern Hemisphere and demonstrated that a detailed understanding of this complex system does not yet exist (Hobbs et al., 2016; Jones et al., 2016). Large-scale observation of Southern Hemisphere sea ice has only been possible since the advent of the satellite era at the end of the 1970s. During this time there has been a statistically significant increase in sea ice extent, dominated by the positive trend in the Western Ross Sea (Hobbs et al., 2016). It has been suggested that the substantial internal variability in the observational record will mask the forced response for several decades (Goosse et al., 2009; Jones et al., 2016). In addition to the substantial interannual variability, the Southern Ocean undergoes an extensive seasonal cycle: each year approximately 15 million square kilometers of ice forms and subsequently melts. The climatology and variability of sea ice in the Southern Ocean are shown in Figure 1c.

The regional response of sea ice to SAM-related forcings has been explored, with some studies showing clear patterns of regionality in sea ice anomalies associated with SAM perturbations (Liu et al., 2004; Simpkins et al., 2012). Other studies have suggested that local winds, which may not be related to the SAM, are more

©2017. The Authors.

This is an open access article under the terms of the Creative Commons Attribution-NonCommercial-NoDerivs License, which permits use and distribution in any medium, provided the original work is properly cited, the use is non-commercial and no modifications or adaptations are made.

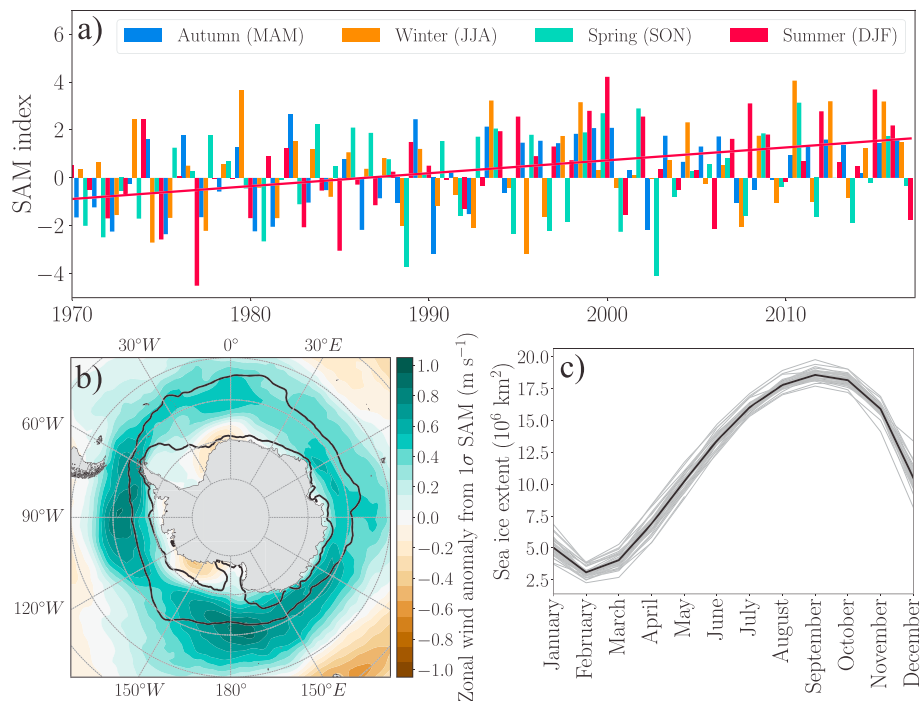


**Figure 1.** The Southern Annular Mode (SAM) and sea ice. (a) The observational record of the SAM in each season from 1970 and the trend line for (December–January–February) DJF SAM (Marshall, 2003); (b) the zonal wind anomaly in January associated with a  $+1\sigma$  DJF SAM from ERA-Interim reanalysis winds (Dee et al., 2011) (colors) along with the 15% sea ice concentration contour during the months of minimum (February) and maximum (September) sea ice extent from satellite data (Reynolds et al., 2002); and (c) the seasonal cycle in sea ice extent, defined as the area covered by ice with a concentration of at least 15%, with individual years shown in gray and the climatology in black (Fetterer et al., 2016).

important (Holland & Kwok, 2012). The difficulties associated with using an annular mode to explain hemispheric sea ice extent changes are exemplified by the record sea ice extents in 2012–2014, which exhibited marked differences in the locations of the sea ice anomalies (Reid & Massom, 2015). Kohyama and Hartmann (2016) explore correlations between modes of atmospheric variability, including the SAM, and variations in sea ice. They find some evidence of the SAM affecting Antarctic sea ice in the Indian Ocean sector during May, June, and July but conclude that sea ice extent is not well explained by the contemporaneous SAM index.

The equilibrium response of sea ice extent to changes in the SAM has been studied using coupled general circulation models, which suggest that an increase in the SAM will lead to a decrease in sea ice extent (Sigmond & Fyfe, 2010, 2013). The link between the SAM and sea ice extent is complicated by the observational record, which shows several decades of increasing SAM (Marshall, 2003) concurrent with an increase in sea ice extent (Parkinson & Cavalieri, 2012; Turner et al., 2013; Zwally, 2002). However, there have been multiple years of record sea ice extent in the past decade (Reid & Massom, 2015), during which there has been no appreciable trend in the SAM (Jones et al., 2016). Multiple studies have found no evidence of a link between the long-term trends in SAM and sea ice extent (Kohyama & Hartmann, 2016; Lefebvre et al., 2004; Simpkins et al., 2012). Ferreira et al. (2015) propose a two time scale response as a solution to this dichotomy; over “short” time scales, an increase in SAM drives an increase in sea ice extent by cooling the sea surface, while eventual upwelling of warmer circumpolar deep water leads to a decrease in sea ice extent over longer time scales (Ferreira et al., 2015; Holland et al., 2016; Kostov et al., 2017).

In this paper we use composites and regression analysis to explore the seasonal response of the Southern Ocean to SAM-related forcings during the austral summer. Due to the link between stratospheric ozone depletion and the DJF SAM, this provides means of exploring possible effects of stratospheric ozone depletion on the seasonal cycle of Antarctic sea ice. Despite the difficulties described previously, and the complexity of the system, we show a robust signal consistent with a simple, physically motivated mechanism. The paper is structured as follows. First, we explore the SST response to SAM anomalies, and then we calculate the effect on sea ice concentration. Following this, we examine the changes in sea ice extent related to summertime

SAM anomalies. In the final section we discuss several individual years and show that this mechanism likely contributed to the negative sea ice extent anomaly observed in early 2017.

## 2. Response to Summertime SAM Anomalies

We consider the seasonal impact of forcings related to summertime SAM anomalies by examining the response of the Southern Ocean using a range of observational data products. These products are an observational SAM index that begins in 1957 (Marshall, 2003), satellite-derived sea surface temperature and sea ice concentration from December 1981 onward (Reynolds et al., 2002), and sea ice extent for the Southern Hemisphere from October 1978 (Fetterer et al., 2016). The seasonal impact of SAM on sea surface temperature and sea ice is assessed using composites and linear regression.

The summertime SAM time series, defined as the seasonal SAM value during December–January–February, is detrended by performing a linear regression and subtracting the linear fit from the data. This gives a time series with a mean of zero and no linear slope. Following Marshall (2003), the year associated with each summertime SAM is the year in which the December occurred. The SST and sea ice concentration data are detrended at each grid point using the same method. The sea ice extent time series is also detrended by removing the linear fit from the data.

The positive SAM composites are constructed by combining years following detrended summertime SAMs larger than 1, while the negative composites combine all years following detrended summertime SAMs less than –1. The negative SAM SST and sea ice concentration composites contain data from 9 years (1983, 1985, 1987, 1992, 2001, 2004, 2006, 2010, and 2017), and the positive composites contain data from 10 years (1982, 1989, 1994, 1995, 1999, 2000, 2002, 2008, 2012, and 2015). Because the sea ice extent record is longer than the other data sets, it begins in late 1978, the sea ice extent composites each contain an additional year; the negative SAM sea ice extent composite contains data from 1980, and the positive SAM composite contains data from 1981. We also analyze sea ice extent with a regression analysis, in which we regress the detrended summertime SAM time series against the detrended monthly sea ice extent data for each calendar month. Thus, the regression slope for each month describes the change in sea ice extent expected from a unit change in the detrended summertime SAM.

In the supporting information we present the results of several additional analyses: composite analysis of the raw SST and sea ice concentration data, and regression analysis applied to both raw and detrended SST and sea ice concentration data. This ensures that our results are not due to any long-term covariability between the variables.

### 2.1. Sea Surface Temperature Response to Summertime SAM

We use the SST composites constructed from the detrended data set to examine the effect of forcings related to the summertime SAM on SST around Antarctica. In the supporting information we show results from a composite analysis using the raw data sets as well as a regression analysis applied to both the raw and detrended data sets.

Positive SAM anomalies during the austral summer months of December–January–February (DJF) are associated with anomalously strong westerly winds. These wind anomalies cause a cooling of the sea surface surrounding Antarctica and warming farther north largely driven by anomalous meridional Ekman transports (Ferreira et al., 2015; Kostov et al., 2017; Purich et al., 2016). Assuming that the thickness of the Ekman layer is equal to or smaller than the depth of the mixed layer, we expect the temporal evolution of the zonal mean SST anomaly,  $\langle \text{SST} \rangle'$ , to be given by

$$\frac{\partial \langle \text{SST} \rangle'}{\partial t} = \frac{\tau_x'}{\rho_0 f h} \frac{\partial \overline{\langle \text{SST} \rangle}}{\partial y} - \lambda \langle \text{SST} \rangle' \quad (1)$$

where  $\langle \text{SST} \rangle'$  is the anomaly in zonal mean sea surface temperature,  $\tau_x'$  is the anomalous zonal wind forcing,  $\rho_0$  is the reference density,  $f$  is the Coriolis parameter,  $h$  is the mixed layer depth,  $\partial \overline{\langle \text{SST} \rangle} / \partial y$  is the meridional derivative of the zonally averaged climatological sea surface temperature, and  $1/\lambda$  is the relaxation time scale associated with damping of SST anomalies. In the absence of damping, the magnitude of the expected response is proportional to the meridional SST gradient and inversely proportional to the mixed layer depth. We use equation (1) as a simple model to understand the temporal evolution of these SST anomalies.

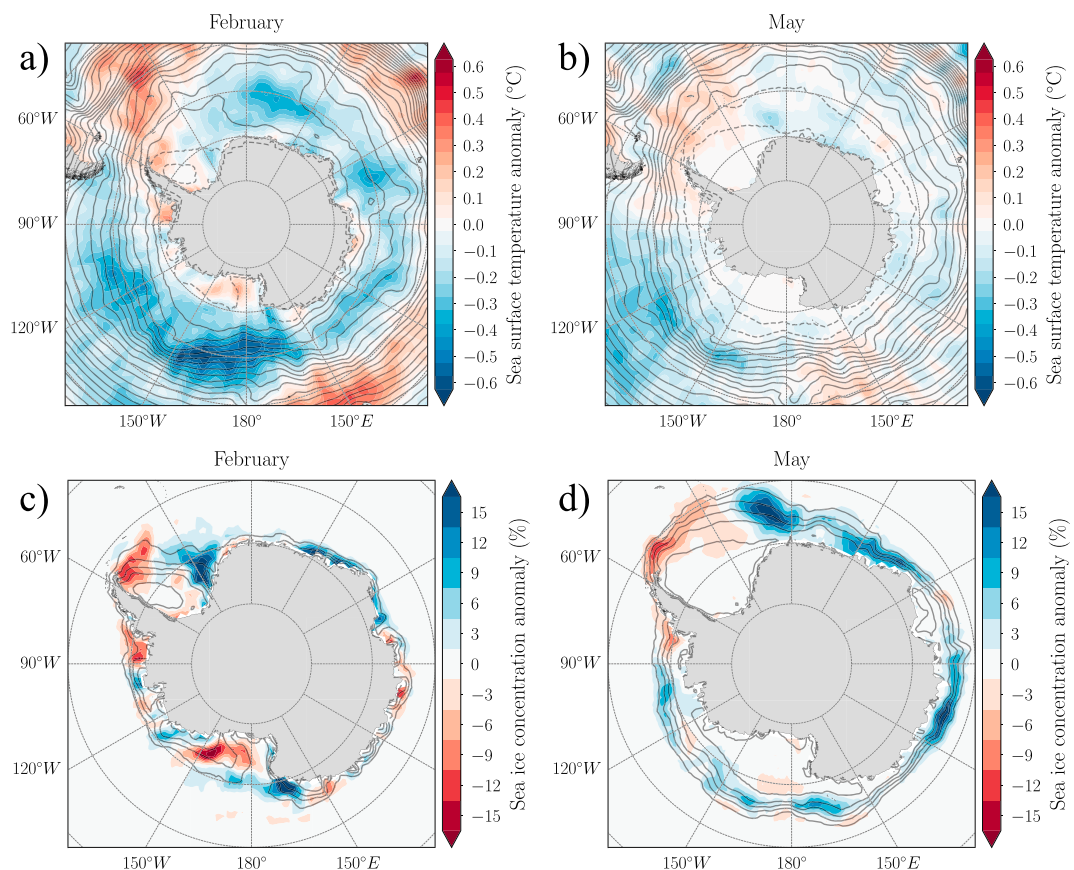


**Figure 2.** Maps of sea surface temperature and sea ice concentration changes in response to DJF SAM-related forcings, calculated as the positive composite minus the negative composite, divided by 2. SST anomalies in (a) February and (b) May, and sea ice concentration anomalies in (c) February and (d) May. The colors show the anomalies while the contours show the climatology. The SST contours are at  $0.5 \pm 1.0, 2.0, \dots, {}^{\circ}\text{C}$  with the negative contours dashed, while the sea ice concentration contours are at 10%, 30%, 50%, 70%, and 90%.

Maps of the SST anomalies from our composite analysis can be seen in Figures 2a and 2b. The temporal evolution of these SST anomalies can be more clearly studied by calculating the mean SST anomaly between  $50^{\circ}\text{S}$  and  $70^{\circ}\text{S}$  from our detrended composites and examining its variation with time. This allows us to examine the magnitude of the initial perturbation and the decay time scale of the induced temperature anomalies. The integrated SST anomalies are shown in Figure 3a as a function of time (note that the negative SAM composite has been multiplied by  $-1$  to aid comparisons between the composites). The integrated SST anomalies differ at a statistically significant level in January ( $p \approx 0.017$ ), February ( $p \approx 0.0012$ ), March ( $p \approx 0.019$ ), and April ( $p \approx 0.023$ ). After May ( $p \approx 0.057$ ) the difference between the composites is not statistically significant using Welch's unequal variances  $t$  test.

The SST anomalies are damped by both atmospheric and oceanic processes. The damping time scale for SST anomalies depends on their latitude and horizontal extent, as well as the season (Hausmann et al., 2016). Of the oceanic processes, the most important is the entrainment of fluid from below the mixed layer as the mixed layer deepens, hence the seasonal dependency in the damping time scale. Consistent with previous studies that have estimated a damping time scale of 3–6 months for large-scale temperature anomalies in the Southern Ocean during the austral autumn (Ciasto & Thompson, 2008; Hausmann et al., 2016), we find a damping time scale of approximately 2.5–3 months (see supporting information). This suggests that SST anomalies may persist for long enough to affect the seasonal cycle of sea ice growth.

## 2.2. Sea Ice Response to Summertime SAM Anomalies

We expect the SST anomalies induced by forcings associated with the SAM to cause changes in the sea ice concentration, with warmer SSTs reducing ice cover and colder SSTs promoting ice. Our analysis shows that autumns following positive DJF SAM anomalies tend to have more sea ice, while autumns following negative

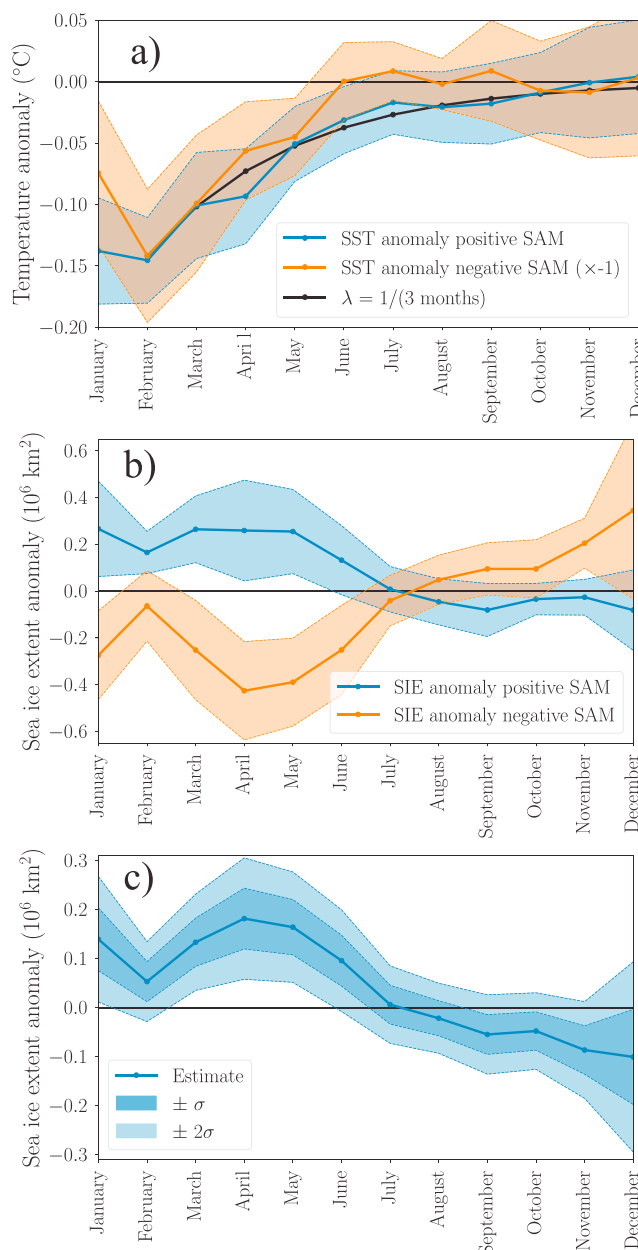


**Figure 3.** Integrated response of sea surface temperature and sea ice to DJF SAM anomalies. (a) Mean temperature anomaly between  $50^{\circ}\text{S}$  and  $70^{\circ}\text{S}$  for the positive and negative SAM composites (the SST values from the negative SAM composite have been multiplied by  $-1$ ). The shaded regions show the standard error of the mean for each composite, given by the standard deviation of the composite divided by the square root of the number of composite members, and the black curve shows an exponential decay with a time scale of 3 months. (b) Evolution of sea ice extent anomaly from the composites. Once again, the shaded regions represent the standard error of the mean. The sea ice extent composites are significantly different in April and May ( $p < 0.05$ ). (c) The expected change in detrended sea ice extent per unit increase in detrended DJF SAM from the regression analysis. The shading represents the uncertainty range encompassed by  $\pm 1$  or  $2$  standard errors of the regression coefficient. The effect is statistically significant in January, March, April, and May ( $p < 0.05$ ).

DJF SAM anomalies generally have less sea ice. The sea ice concentration changes computed from the detrended composites are shown in Figures 2c and 2d.

Changes to the sea ice extent, which is calculated as the area covered by sea ice with a concentration of at least 15%, depend not only on changes in concentration but also on the background state. If there are large areas of ice near this threshold, then small changes in concentration can lead to large changes in extent. Conversely, if the area of sea ice near the 15% cutoff is small, then the change in sea ice extent will also be small. The large year-to-year variation in the spatial distribution of sea ice has complicated previous attempts to explain the impact of SAM-related forcings on sea ice extent (Reid & Massom, 2015). Here we sidestep this issue by focusing on the zonally integrated response of sea ice to SAM anomalies, rather than the regional response.

Following DJF SAM anomalies we find a signal in sea ice extent that persists for many months, as shown in Figures 3b and 3c. Figure 3b shows anomalies of sea ice extent for positive and negative SAM composites relative to the climatological seasonal cycle. During years following a positive DJF SAM sea ice grows more rapidly, while years following a negative DJF SAM show slower ice growth than the climatology. The difference between the two composites is statistically significant in April ( $p \approx 0.034$ ) and May ( $p \approx 0.023$ ), and marginally significant in January ( $p \approx 0.067$ ) and March ( $p \approx 0.060$ ). The shaded regions show the standard error of the mean for each composite. Figure 3c shows the expected change in detrended sea ice extent following a unit increase in the detrended DJF SAM. The change in extent is estimated as the slope of an ordinary least squares regression and is statistically distinguishable from zero in January ( $1.4 \pm 0.6 \times 10^5 \text{ km}^2$  per unit SAM,  $p \approx 0.035$ ), March ( $1.3 \pm 0.5 \times 10^5 \text{ km}^2$  per unit SAM,  $p \approx 0.0098$ ), April ( $1.8 \pm 0.6 \times 10^5 \text{ km}^2$  per unit SAM,  $p \approx 0.0057$ ), and May ( $1.6 \pm 0.6 \times 10^5 \text{ km}^2$  per unit SAM,  $p \approx 0.0059$ ). The error estimate,  $\sigma$ , is the standard error of the regression slope for each month.

The results in Figures 3b and 3c show that following positive SAM anomalies sea ice extent is increased relative to the climatology, while negative SAM anomalies precede anomalously low sea ice extent. The magnitude of this perturbation reaches a maximum in April, before decreasing. Excluding the 2017 data from the analysis reduces the size of the effect, but the signal is still statistically significant in both the regression analysis (April and May) and the composite analysis (May). The fading of the sea ice extent signals over winter is consistent with the assertion that the long-term impact of SAM on sea ice extent is due to subsurface dynamics (Ferreira et al., 2015). Our finding that sea ice extent anomalies due to DJF SAM related forcings do not persist through the winter is also consistent with previous work analyzing the timing of the onset of freezing and thawing in the Southern Ocean (Stammerjohn et al., 2012).

### 3. Individual Years

Figure 4 shows detrended sea ice extent anomalies for all years following a detrended DJF SAM greater than  $1$  or less than  $-1$ . Despite the large amount of variability, there is a clear trend for years following positive SAMs to have more ice, and years following negative SAMs to have less ice, especially during April and May. The sea ice extent curves for four individual years have been labeled. These years correspond to the most extreme January sea ice extent anomalies, and the SAM values are as expected: positive for the positive sea ice extent anomalies and negative for the negative sea ice extent anomalies.

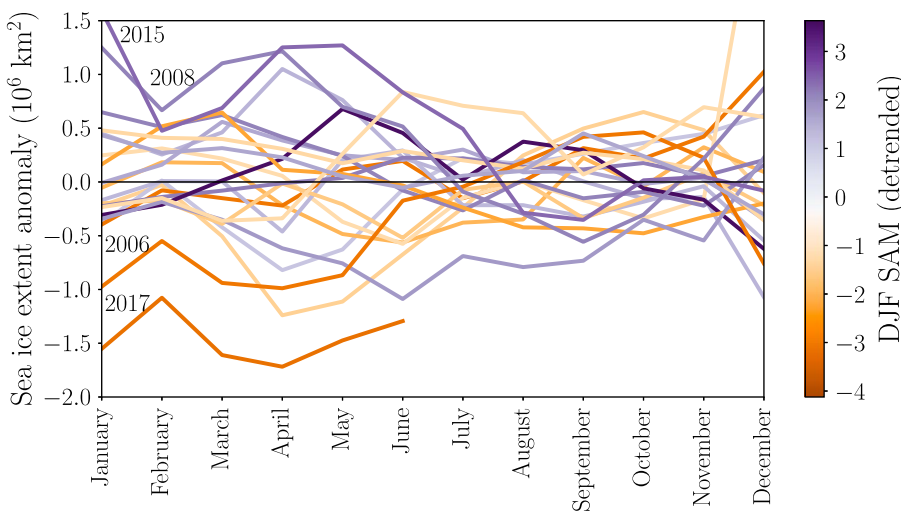


**Figure 4.** The temporal evolution of detrended sea ice extent anomaly for years following detrended DJF SAM values greater than 1 or less than  $-1$ . The two years with very positive sea ice extent anomalies are 2015, following a DJF SAM of 2.4, and 2008, following a DJF SAM of 2.1. The most negative January anomaly is 2017, following a DJF SAM of  $-3.4$ , and 2006, following a DJF SAM of  $-3.0$ .

The detrended summertime SAM in 2016/2017 was a remarkable  $-3.4$ , resulting in anomalously warm SSTs across the Southern Ocean. Based on our regression analysis, we expect this to cause a sea ice extent anomaly of just over  $-0.4 \times 10^6 \text{ km}^2$  in March. The observed anomaly was approximately  $-1.6 \times 10^6 \text{ km}^2$ , which means our mechanism cannot fully explain the observed anomaly. In addition to the negative DJF SAM, the observed SAM was strongly negative in November 2016. It is likely that the wind anomalies associated with this negative November SAM also contributed to the observed record low sea ice extent through the same mechanism we have discussed for the DJF SAM. Our study suggests that the impact of the negative DJF SAM on sea ice extent will likely dissipate by August as the mixed layer deepens, mixing away the warm SST imprint of the SAM: note how the curves in Figure 4 converge by October. Therefore, we expect the magnitude of the current sea ice extent anomaly to continue to decrease as we approach the maximum ice extent in September. Other recent work has suggested that the record minimum sea ice extent in March is the result of multiple storms across the Southern Ocean in the preceding months (Turner et al., 2017). Turner et al. (2017) provide a detailed discussion of snapshots of the atmosphere and their direct impact on local sea ice. The analysis in Turner et al. (2017) and the one we present are complementary. Our analysis describes a mechanism through which a large-scale atmospheric structure, the DJF SAM, is expected to affect sea ice extent in the following months. In contrast, Turner et al. (2017) use the observed state of the atmosphere and previous mechanistic studies relating the atmospheric state with heat fluxes and sea ice dynamics, to explain the observed changes in sea ice.

#### 4. Conclusions

We have used observational data to investigate the impact of DJF SAM-related forcings on sea surface temperature and sea ice during the following year. Our analysis of SST anomalies corroborates earlier results suggesting that the damping time scale for hemispheric SST anomalies near Antarctica is between 3 and 6 months (Ciaist & Thompson, 2008; Hausmann et al., 2016) and suggests that it may be closer to 3 months. Consistent with previous studies we find that anomalies in the SST lead to anomalies in sea ice concentration (Fan et al., 2014).

We find that the seasonal response of sea ice extent to DJF SAM-related forcings is consistent regardless of whether we use regression or composites to analyze the data. The signal is also present in both the raw and the detrended data sets. This provides strong evidence that our results are due to seasonal effects and not long-term covariability between the SAM and sea ice extent. Positive SAM anomalies precede anomalously cold SST around Antarctica and an expansion of sea ice. Negative SAM anomalies precede the opposite response, with warmer SST around Antarctica and a reduction in sea ice extent. In both cases the magnitude of the sea ice extent anomaly reaches a maximum in the autumn. Our regression analysis suggests an increase

of  $1.8 \pm 0.6 \times 10^5 \text{ km}^2$  in detrended April sea ice extent per unit increase in the detrended DJF SAM. Consistent with the results of our analysis, the magnitude of the 2017 detrended sea ice extent anomaly peaked in April and has been decreasing since then. Our results suggest that the magnitude of this anomaly will continue to diminish. The relationship between the summertime SAM and sea ice extent has implications for the seasonal prediction of sea ice extent in future years.

Our study also has implications for the “two time scale” paradigm concerning the response of the Southern Ocean to a step change in the SAM induced by ozone depletion (Ferreira et al., 2015). Our analysis supports the idea that the short time scale response to a positive DJF SAM is one of cooling and sea ice expansion. Kostov et al. (2017) show that the initial cooling response in coupled climate models can build for several years. In our analysis of the observations we do not find evidence of SST or sea ice extent anomalies surviving from 1 year to the next. However, this may be a consequence of the noisy and relatively short nature of the observational record. Due to our focus on the seasonal time scale and detrending of the data, the analysis presented here is ill suited to exploring the longer-term warming response induced by the upwelling of warmer water from beneath the cold, fresh layer at the surface (Ferreira et al., 2015; Kostov et al., 2017).

Previous work has shown a link between anthropogenic ozone depletion and the historical increase in the DJF SAM (see, e.g., Polvani et al., 2011). The results presented in this paper suggest that anthropogenic ozone depletion, by forcing the atmosphere toward a positive SAM state in DJF, may have contributed to a seasonal cooling of SST near Antarctica and an increase in Antarctic sea ice extent during the austral autumn.

#### Acknowledgments

We gratefully acknowledge Dave Thompson for his advice and two anonymous reviewers whose input improved this manuscript. This study was supported by a U.S. National Science Foundation grant of the NSF Antarctic Program. The data that support the findings in this study can be accessed in the following locations: The observational SAM index was downloaded from <http://www.nerc-bas.ac.uk/icd/gjma/sam.html>. NOAA\_OI\_SST\_V2 data were provided by the NOAA/OAR/ESRL PSD, Boulder, Colorado, USA, from their website at <http://www.esrl.noaa.gov/psd/>. The sea ice extent time series, Sea Ice Index V2, was downloaded from the National Snow and Ice Data Center at <ftp://sidads.colorado.edu/DATASETS/NOAA/G02135/south/daily/data/>. ERA-Interim reanalysis winds were obtained from <http://apps.ecmwf.int/datasets/data/interim-full-modas/levtype=sfc/>.

#### References

- Ciasto, L. M., & Thompson, D. W. J. (2008). Observations of large-scale ocean-atmosphere interaction in the Southern Hemisphere. *Journal of Climate*, 21(6), 1244–1259. <https://doi.org/10.1175/JCLI1809.1>
- Dee, D. P., Uppala, S. M., Simmons, A. J., Berrisford, P., Poli, P., Kobayashi, S., ... Vitart, F. (2011). The ERA-Interim reanalysis: Configuration and performance of the data assimilation system. *Quarterly Journal of the Royal Meteorological Society*, 656, 553–597. <https://doi.org/10.1002/qj.828>
- Fan, T., Deser, C., & Schneider, D. P. (2014). Recent Antarctic sea ice trends in the context of Southern Ocean surface climate variations since 1950. *Geophysical Research Letters*, 41, 2419–2426. <https://doi.org/10.1002/2014GL059239>
- Ferreira, D., Marshall, J., Bitz, C. M., Solomon, S., & Plumb, A. (2015). Antarctic Ocean and sea ice response to ozone depletion: A two-time-scale problem. *Journal of Climate*, 28(3), 1206–1226. <https://doi.org/10.1175/JCLI-D-14-00313.1>
- Fetterer, F., Knowles, K., Meier, W., Savoie, M., & Windnagel, A. K. (2016). *Sea Ice Index, version 2*. Boulder, Colorado USA: National Snow and Ice Data Center. <https://doi.org/10.7265/N5736NV7>
- Gong, D., & Wang, S. (1999). Definition of Antarctic oscillation index. *Geophysical Research Letters*, 26(4), 459–462. <https://doi.org/10.1029/1999GL900003>
- Goosse, H., Lefebvre, W., de Montety, A., Crespin, E., & Orsi, A. H. (2009). Consistent past half-century trends in the atmosphere, the sea ice and the ocean at high southern latitudes. *Climate Dynamics*, 33(7–8), 999–1016. <https://doi.org/10.1007/s00382-008-0500-9>
- Hausmann, U., Czaja, A., & Marshall, J. (2016). Estimates of air-sea feedbacks on sea surface temperature anomalies in the Southern Ocean. *Journal of Climate*, 29(2), 439–454. <https://doi.org/10.1175/JCLI-D-15-0015.1>
- Hobbs, W. R., Massom, R., Stammerjohn, S., Reid, P., Williams, G., & Meier, W. (2016). A review of recent changes in Southern Ocean sea ice, their drivers and forcings. *Global and Planetary Change*, 143, 228–250. <https://doi.org/10.1016/j.gloplacha.2016.06.008>
- Holland, M. M., Landrum, L., Kostov, Y., & Marshall, J. (2016). Sensitivity of Antarctic sea ice to the Southern Annular Mode in coupled climate models. *Climate Dynamics*, 1–19. <https://doi.org/10.1007/s00382-016-3424-9>
- Holland, P. R., & Kwok, R. (2012). Wind-driven trends in Antarctic sea-ice drift. *Nature Geoscience*, 5(12), 872–875. <https://doi.org/10.1038/ngeo1627>
- Jones, J. M., Gille, S. T., Goosse, H., Abram, N. J., Canziani, P. O., Charman, D. J., ... Vance, T. R. (2016). Assessing recent trends in high-latitude Southern Hemisphere surface climate. *Nature Climate Change*, 6(10), 917–926. <https://doi.org/10.1038/nclimate3103>
- Kohyama, T., & Hartmann, D. L. (2016). Antarctic sea ice response to weather and climate modes of variability. *Journal of Climate*, 29(2), 721–741. <https://doi.org/10.1175/JCLI-D-15-0301.1>
- Kostov, Y., Marshall, J., Hausmann, U., Armour, K. C., Ferreira, D., & Holland, M. M. (2017). Fast and slow responses of Southern Ocean sea surface temperature to SAM in coupled climate models. *Climate Dynamics*, 48(5–6), 1595–1609. <https://doi.org/10.1007/s00382-016-3162-z>
- Lefebvre, W., Goosse, H., Timmermann, R., & Fichefet, T. (2004). Influence of the Southern Annular Mode on the sea ice—Ocean system. *Journal of Geophysical Research*, 109, C09005. <https://doi.org/10.1029/2004JC002403>
- Liu, J., Curry, J. A., & Martinson, D. G. (2004). Interpretation of recent Antarctic sea ice variability. *Geophysical Research Letters*, 31, L02205. <https://doi.org/10.1029/2003GL018732>
- Marshall, G. J. (2003). Trends in the Southern Annular Mode from observations and reanalyses. *Journal of Climate*, 16(24), 4134–4143. [https://doi.org/10.1175/1520-0442\(2003\)016<4134:TTSAM>2.0.CO;2](https://doi.org/10.1175/1520-0442(2003)016<4134:TTSAM>2.0.CO;2)
- Parkinson, C. L., & Cavalieri, D. J. (2012). Antarctic sea ice variability and trends, 1979–2010. *Cryosphere*, 6(4), 871–880. <https://doi.org/10.5194/tc-6-871-2012>
- Polvani, L. M., Waugh, D. W., Correa, G. J. P., & Son, S.-W. (2011). Stratospheric ozone depletion: The main driver of twentieth-century atmospheric circulation changes in the Southern Hemisphere. *Journal of Climate*, 24(3), 795–812. <https://doi.org/10.1175/2010JCLI3772.1>
- Purich, A., Cai, W., England, M. H., & Cowan, T. (2016). Evidence for link between modelled trends in Antarctic sea ice and underestimated westerly wind changes. *Nature Communications*, 7(10), 409. <https://doi.org/10.1038/ncomms10409>
- Reid, P., & Massom, R. A. (2015). Successive Antarctic sea ice extent records during 2012, 2013, and 2014. In P. Reid, & R. A. Massom (Eds.), *State of the Climate in 2014* (pp. S163–S164). American Meteorological Society. <https://doi.org/10.1175/2015BAMSStateoftheClimate.1>
- Reynolds, R. W., Rayner, N. A., Smith, T. M., Stokes, D. C., & Wang, W. (2002). An improved in situ and satellite SST analysis for climate. *Journal of Climate*, 15(13), 1609–1625. [https://doi.org/10.1175/1520-0442\(2002\)015<1609:AISSAS>2.0.CO;2](https://doi.org/10.1175/1520-0442(2002)015<1609:AISSAS>2.0.CO;2)

- Seviour, W. J., Gnanadesikan, A., Waugh, D., & Pradal, M. A. (2017). Transient response of the Southern Ocean to changing ozone: Regional responses and physical mechanisms. *Journal of Climate*, 30(7), 2463–2480. <https://doi.org/10.1175/JCLI-D-16-0474.1>
- Seviour, W. J. M., Gnanadesikan, A., & Waugh, D. W. (2016). The transient response of the Southern Ocean to stratospheric ozone depletion. *Journal of Climate*, 29(20), 7383–7396. <https://doi.org/10.1175/JCLI-D-16-0198.1>
- Sigmond, M., & Fyfe, J. C. (2010). Has the ozone hole contributed to increased Antarctic sea ice extent? *Geophysical Research Letters*, 37, L18502. <https://doi.org/10.1029/2010GL044301>
- Sigmond, M., & Fyfe, J. C. (2013). The Antarctic sea ice response to the ozone hole in climate models. *Journal of Climate*, 27, 1336–1342. <https://doi.org/10.1175/JCLI-D-13-00590.1>
- Simpkins, G. R., Ciasto, L. M., Thompson, D. W. J., & England, M. H. (2012). Seasonal relationships between large-scale climate variability and Antarctic sea ice concentration. *Journal of Climate*, 25(16), 5451–5469. <https://doi.org/10.1175/JCLI-D-11-00367.1>
- Stammerjohn, S., Massom, R., Rind, D., & Martinson, D. (2012). Regions of rapid sea ice change: An inter-hemispheric seasonal comparison. *Geophysical Research Letters*, 39, 1–8. <https://doi.org/10.1029/2012GL050874>
- Thompson, D. W. J., & Wallace, J. M. (2000). Annular modes in the extratropical circulation. Part I: Month-to-month variability. *Journal of Climate*, 13(5), 1000–1016. [https://doi.org/10.1175/1520-0442\(2000\)013<1000:AMITEC>2.0.CO;2](https://doi.org/10.1175/1520-0442(2000)013<1000:AMITEC>2.0.CO;2)
- Turner, J., Bracegirdle, T. J., Phillips, T., Marshall, G. J., & Scott Hosking, J. (2013). An initial assessment of Antarctic sea ice extent in the CMIP5 models. *Journal of Climate*, 26(5), 1473–1484. <https://doi.org/10.1175/JCLI-D-12-00068.1>
- Turner, J., Phillips, T., Marshall, G. J., Hosking, J. S., Pope, J. O., Bracegirdle, T. J., & Deb, P. (2017). Unprecedented springtime retreat of Antarctic sea ice in 2016. *Geophysical Research Letters*, 44, 6868–6875. <https://doi.org/10.1002/2017GL073656>
- Zwally, H. J. (2002). Variability of Antarctic sea ice 1979–1998. *Journal of Geophysical Research*, 107, C53041. <https://doi.org/10.1029/2000JC000733>